PROCEEDINGS OF SPIE

SPIEDigitalLibrary.org/conference-proceedings-of-spie

High-throughput processes and structural characterization of single-nanotube based devices for 3D electronics

A. B. Kaul, K. G. Megerian, R. L. Baron, A. T. Jennings, D. Jang, et al.

A. B. Kaul, K. G. Megerian, R. L. Baron, A. T. Jennings, D. Jang, J. R. Greer, "High-throughput processes and structural characterization of single-nanotube based devices for 3D electronics," Proc. SPIE 7318, Micro- and Nanotechnology Sensors, Systems, and Applications, 73180B (11 May 2009); doi: 10.1117/12.820723

SPIE.

Event: SPIE Defense, Security, and Sensing, 2009, Orlando, Florida, United States

Downloaded From: https://www.spiedigitallibrary.org/conference-proceedings-of-spie on 5/30/2018 Terms of Use: https://www.spiedigitallibrary.org/terms-of-use

High-throughput processes and structural characterization of single-nanotube based devices for 3D electronics

A. B. Kaul[(a)], K. G. Megerian, and R. L. Baron
Jet Propulsion Laboratory, California Institute of Technology, Pasadena, CA 91109

A. T. Jennings, D. Jang, and J. R. Greer
Division of Engineering and Applied Science, California Institute of Technology, Pasadena, CA 91125

ABSTRACT

We have developed manufacturable approaches to form single, vertically aligned carbon nanotubes, where the tubes are centered precisely, and placed within a few hundred nm of 1-1.5 μm deep trenches. These wafer-scale approaches were enabled by chemically amplified resists and inductively coupled Cryo-etchers to form the 3D nanoscale architectures. The tube growth was performed using dc plasma-enhanced chemical vapor deposition (PECVD), and the materials used for the pre-fabricated 3D architectures were chemically and structurally compatible with the high temperature (700 ºC) PECVD synthesis of our tubes, in an ammonia and acetylene ambient. The TEM analysis of our tubes revealed graphitic basal planes inclined to the central or fiber axis, with cone angles up to 30º for the particular growth conditions used. In addition, bending tests performed using a custom nanoindentor, suggest that the tubes are well adhered to the Si substrate. Tube characteristics were also engineered to some extent, by adjusting growth parameters, such as Ni catalyst thickness, pressure and plasma power during growth.

1. INTRODUCTION

The constant drive toward miniaturization driven primarily by the microelectronics industry has created niche opportunities for nanoscale materials, such as carbon nanotubes that show promise as interconnects,[1] novel transistors,[2] or heat transport materials.[3] A heavily utilized technique for the synthesis of carbon nanotubes, specifically multi-walled-nanotubes (MWNTs), is thermal chemical vapor deposition (CVD), which results in 'bundles' of tubes largely perpendicular to the substrate. Inspection of MWNTs in such bundles reveals individual tubes growing in random directions and forming a 'matted' array. Often, this poor vertical tube alignment does not maximally utilize the exceptional 1D thermal, mechanical, electrical or optical properties of the tubes,[4] and reduces performance for certain applications, such as field emitters[5] for flat panel displays, or thermal interface materials for integrated circuits.[6]

A technique which has emerged in recent years to ensure excellent vertical tube alignment is plasma-enhanced (PE)-CVD,[7] where the inherent E-field in the plasma allows tube growth in a direction parallel to the field. Analysis of crystallinity of individual tubes reveals graphitic structures where the graphene

[(a)]Email: anupama.b.kaul@jpl.nasa.gov
Copyright 2009 California Institute of Technology. Government Sponsorship is acknowledged.

Micro- and Nanotechnology Sensors, Systems, and Applications, edited by Thomas George, M. Saif Islam, Achyut K. Dutta, Proc. of SPIE Vol. 7318, 73180B · © 2009 SPIE · CCC code: 0277-786X/09/$18 · doi: 10.1117/12.820723

Downloaded From: https://www.spiedigitallibrary.org/conference-proceedings-of-spie on 5/30/2018 Terms of Use: https://www.spiedigitallibrary.org/terms-of-use

layers are inclined to the central axis,[8] structures commonly referred to as carbon nanofibers (CNFs); however, control over their physical orientation with the plasma is excellent. Various plasma sources have been employed for tube or CNF growth, such as microwave, inductively coupled plasma (ICP), dc and dc with hot filament; a comprehensive review of the PECVD technique for tube synthesis is provided by Melechko, *et al.*[9]

Besides the ability to direct growth orientation, another important figure of merit for many applications is the precise control over tube placement. There have been many reports on the PECVD growth of multiple tubes formed at controlled locations using positive tone novalac/diazoquinone-based or negative tone rubber/azide resists. When only single tubes are desired where the catalyst size has to be controlled below a few hundred nm, such resist systems show excessive absorption in the deep-UV region, and are inadequate for deep-submicron feature size resolution. To date, e-beam lithography has been the main technique implemented for catalyst definition for the realization of arrays of individual, free-standing, vertically aligned CNTs or CNFs using PECVD.[10] However, e-beam lithography is slow and expensive, and ultimately limits the transition of nanoscale devices from the laboratory into commercial production. Moreover, in reports to date, single, vertically aligned tubes formed with PECVD have typically been grown on planar 2D substrates. In this paper, we describe approaches to form single, vertically aligned tubes in 3D nanoscale architectures using high throughput nanomanufacturable techniques, where chemically amplified polyhydroxystyrene resin-based deep UV resists are employed for deep submicron feature size resolution.[11]

Such resist systems, coupled with state-of-the-art high density, low pressure ICP plasma etching techniques afford top-down approaches for forming high aspect ratio, nanoscale structures, which can then be integrated with PECVD grown tubes. We will describe the approaches developed in order to precisely control and integrate single, aligned PECVD grown nanotubes into such architectures using low-cost, high-throughput wafer-scale techniques that should accelerate development of PECVD grown tubes for a broad range of applications, such as nano-electro-mechanical-systems (NEMS), interconnects, sensors, and 3D electronics in general.

For many device applications, it is also important to gain better insight into the structural characteristics of our PECVD synthesized tubes. We have performed structural characterization of our tubes using Transmission Electron Microscopy (TEM), in addition to initiating nano-mechanical bending tests that shed some insight on factors such as tube-to-substrate adhesion. In addition, techniques for engineering tube characteristics via CVD growth parameters, such as pressure, catalyst thickness and plasma power will also be presented.

2. TUBE SYNTHESIS PROCEDURE

A schematic of our load-lock based PECVD growth chamber is provided elsewhere.[12] The starting substrate was typically a degenerately doped Si wafer (1 - 5 mΩ-cm) with pre-patterned features on it. After Ni catalyst deposition, a pretreatment step was typically carried out for 1-2 min. prior to CNT growth, where a low power hydrogen plasma (60 W, 5 Torr) reduced the surface oxide on the Ni at 700 ºC. Following pretreatment, the chamber was pumped out until the pressure was restored to ~ 2 x 10^{-6} Torr, after which point high purity acetylene (C_2H_2) and ammonia (NH_3) were introduced, which served as the carbon feedstock and diluent gas, respectively. When the desired growth pressure had been attained, the dc discharge was ignited, and growth was carried out for a fixed duration. After completion, the samples were immediately transferred into the load lock for cooling and imaged using the SEM (JEOL-6700F).

Downloaded From: https://www.spiedigitallibrary.org/conference-proceedings-of-spie on 5/30/2018 Terms of Use: https://www.spiedigitallibrary.org/terms-of-use

3. RESULTS AND DISCUSSION

3.1 E-field Aligned Growth

When only C_2H_2 and NH_3 were present at a temperature of ~ 700 ºC in the absence of an electric field, unaligned tubes resulted, as shown in Fig. 1a. In the presence of a stable plasma, a ~ 15 nm thick Ni catalyst resulted in a large areal density of vertically aligned tubes, as shown in the SEM in Fig. 1b.

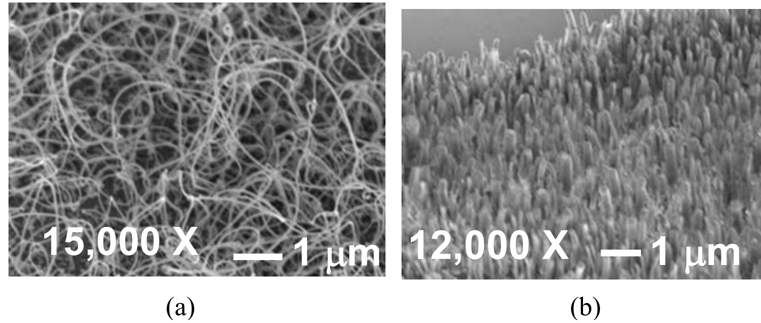

Figure 1. (a) Unaligned tubes result when C_2H_2 and NH_3 are used in the absence of an E-field. (b) A high areal density of vertically aligned tubes was achieved using a 15 nm thick Ni film on degenerately doped Si, with 53 sccm of C_2H_2 and 90 sccm of NH_3 at 5 Torr and 300 mA.

3.2 Step-and-repeat Deep UV Optical Lithography and ICP Cryo-etching

While a large density of vertically aligned tubes was evident using dc PECVD on a continuous Ni film, the position selective growth of CNTs is important for applications where tube growth is desired at only certain locations. Positive tone novalac/diazoquinone-based or negative tone rubber/azide-based resists have been used to form multiple tubes with PECVD at selected locations. In order to form single tubes, it has been determined that a catalyst diameter below about 300 – 400 nm is necessary.[10] E-beam lithography has typically been used to define the catalyst film when single tubes are desired, but this technique is limited by low processing speed and high cost, posing a severe impediment to applications and manufacturability.

We initiated the growth of single, vertically aligned tubes using dc PECVD, where a deep UV (λ = 248 nm) eximer laser lithography tool (Canon FPA-3000 EX3 stepper) was used in conjunction with chemically amplified polyhydroxystyrene resin-based deep UV resists to pattern Ni catalyst dots in the few hundred nm diameter range. Other top down techniques exist, such as the use of self-assembled nanoshpere lithography, which yields periodic arrays of dots in the 30-200 nm range, where the polystyrene nanospheres act as a mask for catalyst deposition.[13] However such techniques are limited to planar 2D substrates, where the tubes are nucleated specifically in periodic arrays, and cannot be used for applications where a single, isolated tube may be desired, or one where pre-patterned features exist.

The structural characterization of the Ni dots after lift-off in acetone revealed a high yield of 300 nm wide Ni catalyst dots in the array, as indicated by the SEM image in Fig. 2a; catalyst dots such as these nucleated predominately single tubes, as depicted in Fig. 2b. The ~ 2 μm long tubes were also self-supporting and generally aligned, unlike tubes formed using thermal CVD that grow in random orientations.

Downloaded From: https://www.spiedigitallibrary.org/conference-proceedings-of-spie on 5/30/2018 Terms of Use: https://www.spiedigitallibrary.org/terms-of-use

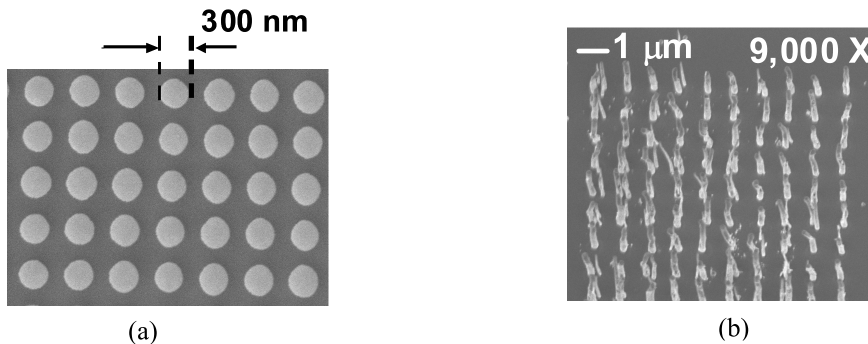

Figure 2. (a) Top-view SEM scan of 300 nm wide Ni dot array formed using chemically amplified AZ 8250 resist, and deep UV (λ = 248 nm) optical lithography. (b) Single ~ 2 μm long vertically aligned tubes nucleated from catalyst arrays such as those in (a). Tilt angle in (b) is ~ 30º.

A variety of applications can emerge in 3D electronics, when isolated PECVD grown tubes can be integrated with 3D nanoscale architectures, such as electrodes that are within a few hundred nm of the tubes. We describe approaches that utilize high throughput, top-down nano-manufacturable techniques to form high aspect ratio 3D nanoscale architectures that are integrated with single, vertically aligned PECVD grown tubes.

The electrodes consisted of bilayer stacks of either degenerately doped ~ 1.0 μm thick Si Device layer, over a 0.5 μm Burried-Oxide (BOX) layer on Silcon-On-Insulator (SOI), or a deposited Nb film on thermal SiO_2 (0.8 μm/0.4 μm). The stack, with an electrode width of ~ 0.4 μm – 1.0 μm, was to be etched 1 - 1.5 μm down to the degenerately doped Si substrate, where tube growth was to be initiated using dc PECVD. A positive tone, chemically amplified resist, AZ 8250, was used to define the electrodes, but maintaining a vertical etch profile with minimal undercut of such high aspect ratio features required substantial optimization of etch chemistries.

Low pressure, high density plasmas have proven advantageous for defining small features precisely using the Deep-trench Reactive Ion Etching (DRIE) or the so-called BOSCH process.[14] In contrast, cryogenic etching, or Cryo-DRIE first proposed by Taichi[15] is becoming increasingly popular compared to the standard BOSCH process. In the BOSCH process, a fluorocarbon polymeric inhibitor layer is formed with C_4F_8 plasma chemistry, for sidewall protection in order to fabricate high aspect ratio microstructures. In contrast, the Cryo-DRIE process utilizes a non-polymeric inhibitor layer for low-bias, fluorine ICP plasmas, which can be removed easily compared to a polymeric inhibitor layer. We implemented the Cryo-DRIE technique for the realization of our high aspect ratio electrodes.

The Si etching experiments were carried out in a Unaxis Fluorine ICP reactor (P-6857). In 100 % SF_6 a severe undercutting of the Si electrodes was observed, as indicated by the SEM in Fig. 3a; decomposition of SF_6 produces F radicals that etch silicon spontaneously due to the exothermic nature of the reaction, which forms volatile SiF_4. The etching conditions had to be optimized in order to form high structural integrity electrodes with minimal undercut. This was achieved with the addition of O_2 to SF_6, which formed highly anisotropy Si electrodes, shown in Fig. 3b, with a Si etch rate of ~ 1.1 μm/min. Moreover, unlike the BOSCH process operated in the time multiplexed mode, sidewall rippling was absent in Cryo-DRIE, since the sidewalls appear smooth. If the oxygen content is exceeded however, etch rates were reduced substantially, with the added possibility of forming black Si. The Cryo-DRIE process relies on the high sticking coefficient of oxygen on the silicon surface at low temperatures, where the substrate is cooled by a He chuck, which enhances the formation of the SiO_xF_y passivation layer, and minimizes lateral etch rates. At such low temperatures, the probability of fluorine radicals reacting with Si is also reduced, which decreases the chemical contribution to the etching.

Downloaded From: https://www.spiedigitallibrary.org/conference-proceedings-of-spie on 5/30/2018 Terms of Use: https://www.spiedigitallibrary.org/terms-of-use

Similarly, we have experimented with etching thick metal films, such as Nb (~ 0.8 μm) using ICP etchers to control undercut, to form near-vertical sidewalls of high aspect ratio electrodes for their integration with the PECVD grown nanotubes. Again, severe pattern distortion was observed in a fluorine ICP etch chemistry, as shown by the electrodes in Fig. 3c. A Unaxis Chlorine ICP etcher (P-6692) was then utilized, where the ratio of BCl_3 and Cl_2 was controlled carefully to form smooth sidewalls -- primarily attributed to BCl_3 -- without compromising etch rates -- determined mainly by the ratio of Cl_2. This etch also showed excellent selectivity toward the underlying oxide. After the etch was complete, the wafer was recoated with AZ 8250 resist for performing the oxide etch in a CHF_3/O_2 plasma chemistry, which also showed good selectivity toward the underlying Si layer. The layer-to-layer registration was excellent and the SEM image in Fig. 3d depicts electrodes with smooth, vertical sidewalls and excellent structural integrity.

With electrode etch chemistries optimized, the objective now was to control tube growth processes such that the tubes were precisely centered within electrodes such as Fig. 3d, by defining a Ni catalyst dot in the region between the electrodes.

In order to pattern a ~ 300 nm dot at the bottom of a 1- 1.5 μm deep trench, and at the same time having a sufficiently thick resist layer to lift-off Ni easily, pushes the limits of what is feasible with wafer-scale approaches such that high-resolution and high-registration are still maintained. The resist stack had to be engineered carefully in order to meet these competing requirements. The ability of the Canon Stepper to offset the optimal focus at some depth away from the surface was also very important. A negative tone chemically amplified resist, UVN 30 was used to pattern the catalyst. However, this resist alone was too thin (< 1 μm), and did not cover the stack adequately. An under layer of PMMA was then used whose viscosity had to be optimized in order to form a ~ 0.7 μm thick layer, which simply acted as a mechanical buffer to planarize the trenches to some extent. The photosensitive UVN layer was then spun on, and features sizes down to 300 nm were defined optically onto the resist layer. Physical etching in an oxygen plasma was then used to transfer the pattern into the PMMA layer.

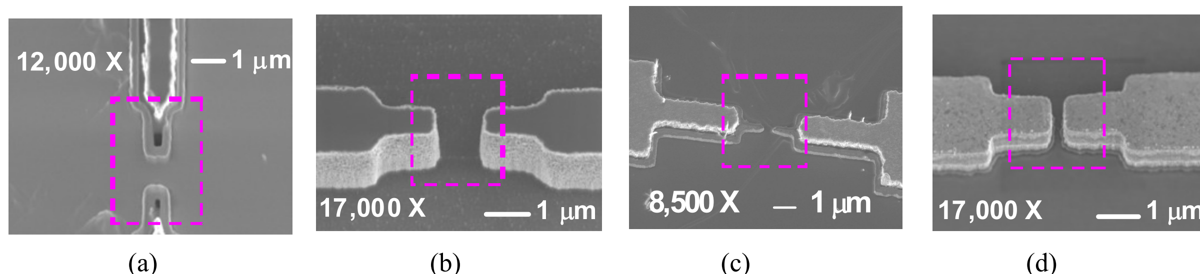

Figure 3. Despite the ability to lithographically pattern nano-scale features, unoptimized etch chemistries can cause severe pattern distortion. a) Si electrode etched in 100 % SF_6 using a Fluorine ICP etcher, revealing severe undercutting of electrodes as viewed from the top. (b) Processes were developed to form high integrity Si electrodes using a combination of SF_6/O_2 chemistries using Cryo-DRIE at 10 mTorr, 400 W ICP power, 100 W bias power, 80 sccm SF_6 and 40 sccm O_2. Sidewall rippling was absent as is conventionally seen with the BOSCH process. (c) Similarly, Nb metal electrodes were severely distorted in an etch chemistry of $CCl_2F_2/CF_4/O_2$. (d) Chlorine ICP etch chemistries were optimized that resulted in minimal undercut of high aspect ratio, nano-scale structures, without compromising etch rates or selectivity (10 mTorr, 15 sccm BCl_3, 20 sccm Cl_2, 400 W ICP power, 100 W bias power). Tilt angle for (c) and (d) above was 20º.

The Ni film was then e-beam evaporated to a thickness ranging from 5 – 15 nm, and the UVN 30/PMMA stack was lifted off in acetone. Shown in Fig. 4a is the wafer after Ni lift-off, which reveals a 300 nm catalyst dot at the bottom of the 1.2 μm trench, where the registration marks in Fig. 4b, indicates

Downloaded From: https://www.spiedigitallibrary.org/conference-proceedings-of-spie on 5/30/2018 Terms of Use: https://www.spiedigitallibrary.org/terms-of-use

excellent layer-to-layer registration (3σ overlay tolerance < 50 nm). Therefore, besides the ability to resolve few hundred nm features within deep trenches, the alignment accuracy of the Canon Stepper was extremely attractive for such multi-layer processes with stringent alignment requirements.

After the catalyst dot was defined, the sample was then ready for CNT growth, where the Nb/SiO_2 electrodes were used. Shown in Fig. 5a is a low magnification SEM image that depicts two Nb/SiO_2 electrodes. The high magnification image in Fig. 5b reveals a single, vertically aligned CNT that is centered, and within ~ 300 nm of ~ 1.2 μm tall electrodes on either side. This is the first report where single, vertically aligned PECVD grown tubes have been integrated with 3D nanoscale architectures using techniques that are completely amenable to high throughput, low cost nano-manufacturability, in contrast to e-beam lithography typically used.

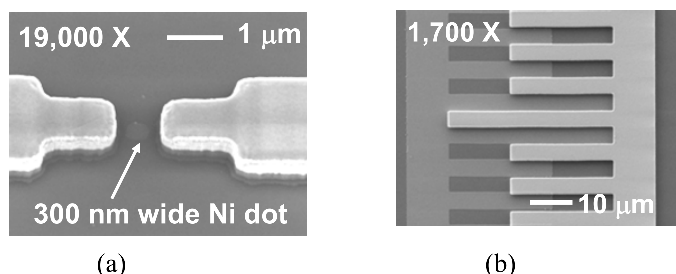

(a) (b)

Figure 4. (a) Shown is a 300 nm Ni catalyst dot centered at the bottom of a 1.2 μm deep trench, with the corresponding registration marks in (b) indicating excellent layer-to-layer alignment.

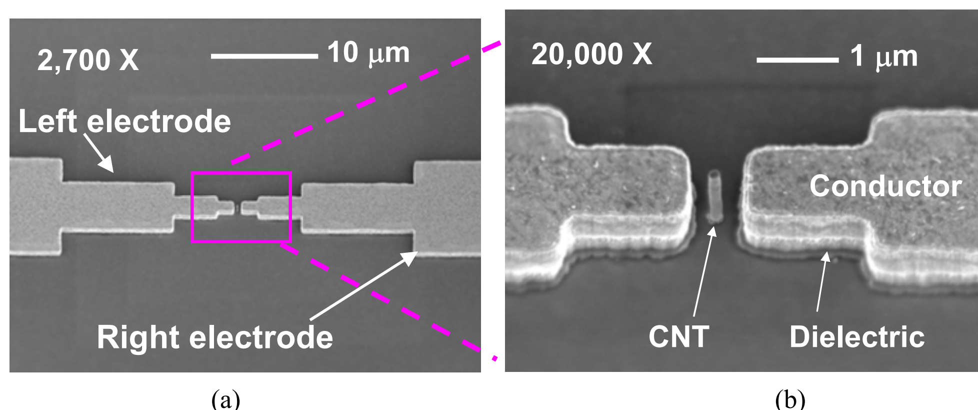

(a) (b)

Figure 5. (a) The low magnification image on the left shows electrodes on either side, and (b) the high magnification image depicts a single, vertically aligned tube centered and < 300 nm away from the electrode that resulted from a typical catalyst dot, such as in Fig. 4a. The growth pressure used was 5 Torr with a 15 nm thick Ni. The processes developed are amenable to high throughput nano-manufacturability, and incorporate both top-down fabrication and bottom-up synthesis.

3.3 Structural Characterization and PECVD Synthesis of Tubes

For the SEM images of Fig. 5, the growth conditions used resulted in 200-250 nm wide tubes. For certain applications, tube characteristics may need to be engineered, such as the extent to which they emerge above the electrodes, or their diameters, which changes their mechanical properties. These characteristics were controlled to some extent, by adjusting the CVD growth parameters, such as growth pressure, catalyst thickness, and power. As an example, the SEM in Fig. 6a shows tubes of diameters

Downloaded From: https://www.spiedigitallibrary.org/conference-proceedings-of-spie on 5/30/2018 Terms of Use: https://www.spiedigitallibrary.org/terms-of-use

ranging from 200 nm down to only 40 nm, which resulted from varying CNT growth parameters. Also, as is evident from this figure, a tip growth mechanism was operative, where the nominally pear-shaped[16] nickel cap, remains on the tip as the tube grows.

Structural characterization of the tubes was also conducted using the FEI Tecnai-F20 scanning transmission electron microscope (STEM) which has a field emission source up to 200 kV. TEM analysis of the mechanically transferred tubes grown directly on Si reveals a structure where the graphite basal planes are inclined to the central or tube axis, where this inclination or cone angle is denoted by θ (Figs. 6b and 6c). Such a configuration, also referred to as the herring bone structure, is generally common with PECVD generated tubes and is perhaps more clearly illustrated by the schematic in Fig. 6d.[17] From this analysis θ of up to 30º was determined for these particular tubes (Fig. 6c), but it can vary as a result of the growth conditions. For example, θ is found to increase as the hydrogen content during CNT growth (in our case NH_3 is the hydrogen carrying gas) is increased.[8]

Mechanical testing of the tubes was also conducted using a custom built nanoindentor inside an SEM, known as the Sementor.[18] A Berkovich tip was used to indent a forest of tubes as shown in Fig. 6e. The SEM image taken for a forest after indentation (Fig. 6f) reveals that the tubes fracture at the base, but do not necessarily detach from the substrate. These measurements suggest that the adhesion of the tubes to the Si substrate is quite strong. Further experiments are currently in progress to better quantify these parameters, in addition to determining other materials properties that are of interest for device applications.

A parametric investigation of the tube growth parameters (pressure, catalyst thickness and power) was also performed and the effect on the physical tube characteristics was analyzed. The tube growth rate was seen to increase with increasing pressure up to about 10 Torr, after which point it saturated, as shown in Fig. 7a. The growth model for PECVD tubes[16,19] suggests decomposition of hydrocarbons at the catalyst surface causing carbon adsorption, which is followed by surface and bulk diffusion of carbon into the nanoparticle. Precipitation of carbon from the supersaturated nanoparticle results in nanotube growth at the tip. It is likely that an increase in pressure causes the surface and bulk diffusion constants to increase, causing the tube growth rate to also increase with pressure. However, at sufficiently high pressure, growth rate is saturated possibly due to the carbon solid solubility limit, where the extra carbon within the nanoparticle can deposit directly on the Ni surface; this would prevent subsequent diffusion and limit growth rate. Chowalla *et al.*[20] noticed a linear increase in growth rate with pressure as we have observed here, however they do not report on pressures beyond ~ 10 Torr.

The thickness of the Ni catalyst layer strongly affected the physical characteristics of the resulting tubes, as shown by the plot in Fig. 7b. These results suggest that a thin Ni catalyst film (~ 5 nm) nucleated tubes that were thinner and longer, while a catalyst film that was thick (~ 15 nm) nucleated tubes that were shorter and wider. Such findings appear to agree with earlier reports.[7,20] The ensuing carbon volume was plotted as a function of catalyst thickness, as shown in Fig. 7c, where the carbon volume was derived from the measured tube dimensions (approximating the tube as a filled cylinder). Interestingly, a maximum in carbon volume was attained at a catalyst thickness of ~ 10 nm; the significance of this result is yet to be analyzed in detail, but may have to relate to the Ni nanocluster size that is created from thermodynamic and kinetic driving forces.

The effect of plasma power on tube growth was also explored, and is shown in Fig. 7d. The dc supply was operated in constant current mode and the power was computed based on the voltage drop between the cathode and anode. It shows that for low powers below about 140 W, the growth rate was significantly reduced, with little change beyond this point up to about 240 W. This is likely due to the plasma chemistry, where the degree of gas dissociation is determined by the power. In general, engineering tube characteristics via growth parameters can further aid in the application of PECVD tubes with desirable characteristics to be integrated into 3D nanoscale architectures.

Downloaded From: https://www.spiedigitallibrary.org/conference-proceedings-of-spie on 5/30/2018 Terms of Use: https://www.spiedigitallibrary.org/terms-of-use

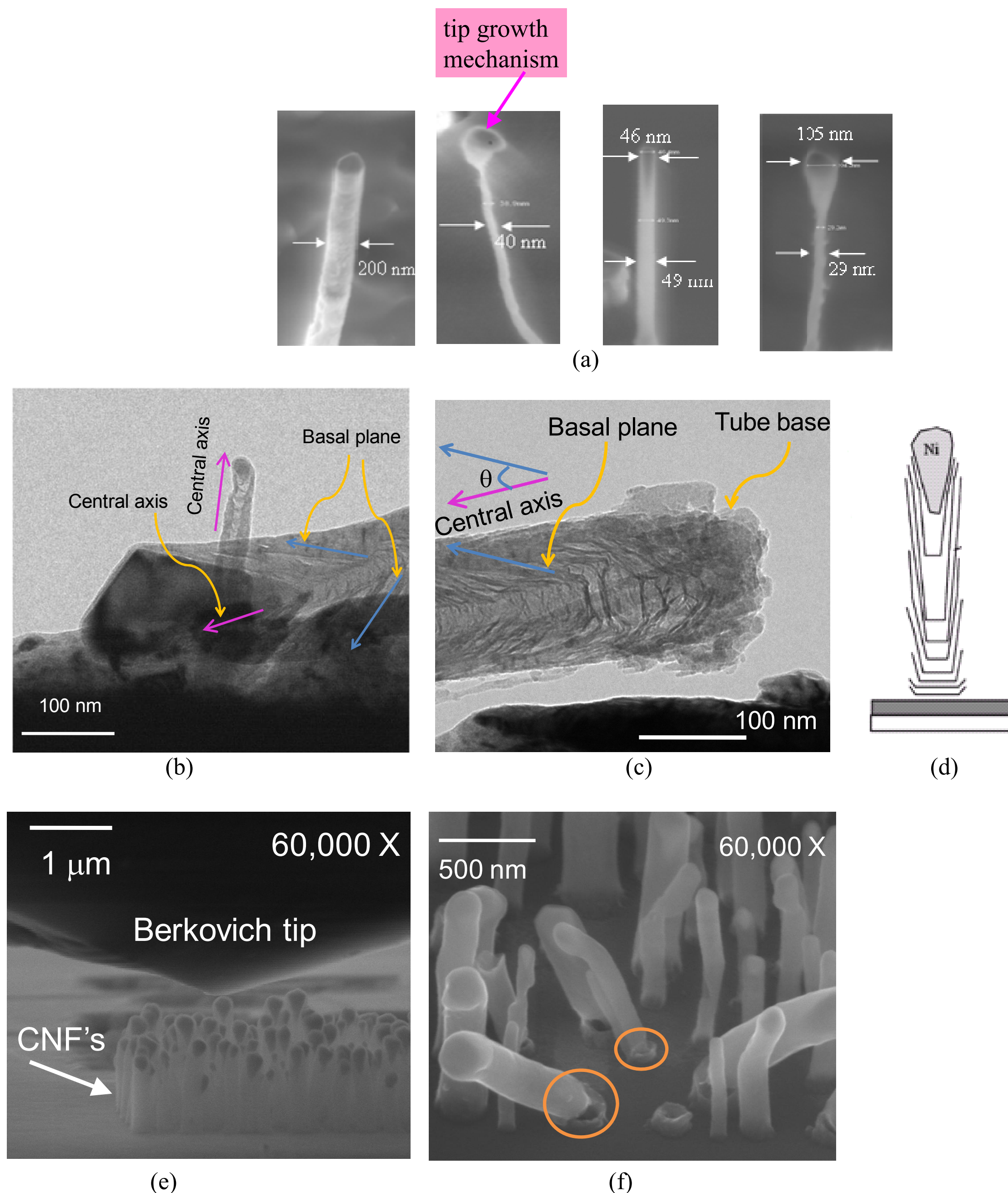

Figure 6. (a) Tube characteristics were engineered to some extent, via CNT growth parameters (pressure, catalyst thickness and power) and depict very wide ~ 200 nm tubes down to tubes only ~ 29 nm wide. A tip growth mechanism was also seen to be operative for Ni/Si. (b) TEM image of two CNFs indicating the direction of the graphite basal planes relative to the central axis. (c) A cone angle θ of up to ~ 30° was determined for this tube. (d) Schematic taken from Ref. 17 which more clearly illustrates the structure of such Ni catalyzed CNFs. (e) A Berkovich tip is used to mechanically bend a forest of tubes in a Sementor (Ref. 18). (f) An SEM image of tubes taken after the mechanical bending tests, which indicates the tubes fracture at the base and do not necessarily detach from the substrate, suggesting the tube-to-substrate adhesion is strong.

Downloaded From: https://www.spiedigitallibrary.org/conference-proceedings-of-spie on 5/30/2018 Terms of Use: https://www.spiedigitallibrary.org/terms-of-use

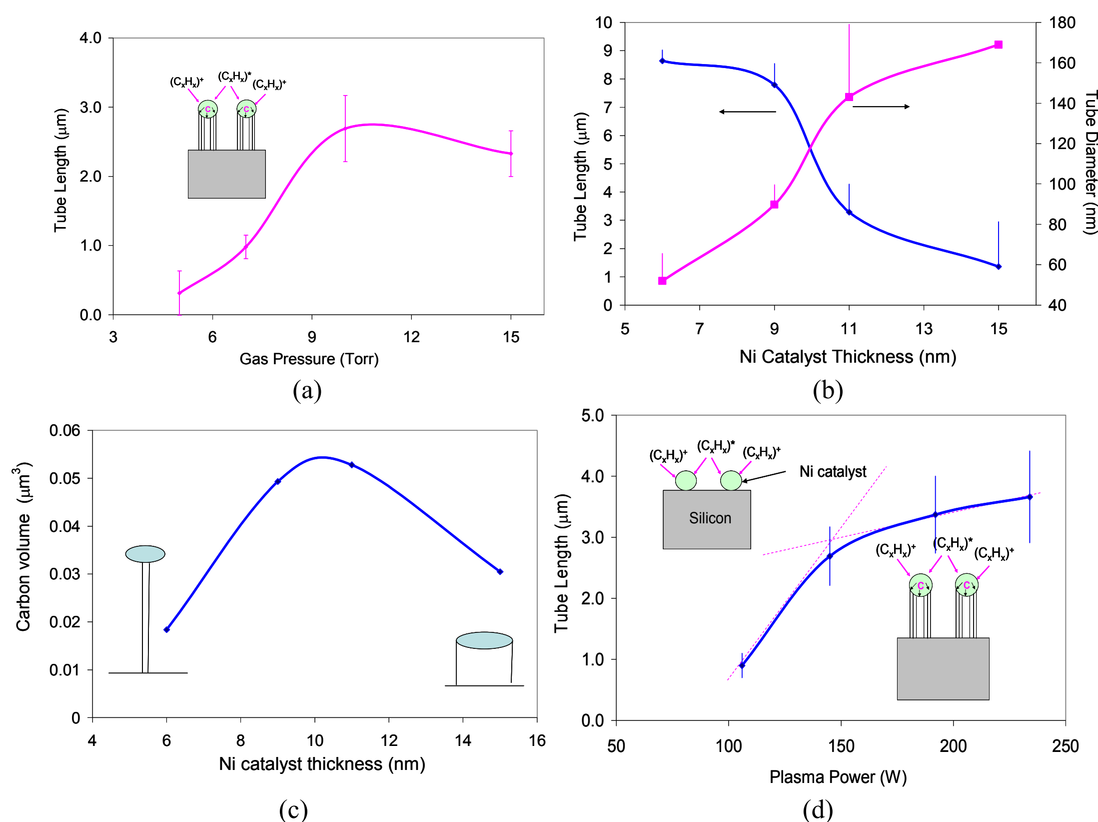

Figure 7. (a) Tube length as a function of pressure shows a near linear increase up to about 10 Torr, beyond which growth rate saturates. Conditions were 22 sccm C_2H_2, 90 sccm NH_3, 9 nm Ni thickness, 400 mA plasma current, and 6 min. growth time. (b) Tube length and diameter as a function of Ni catalyst thickness which suggests thin catalyst layers (e.g. ~ 5 nm) nucleate narrow and long tubes, while thicker catalyst layers (e.g. 15 nm) nucleate short and wide tubes. Growth conditions were 22 sccm C_2H_2, 90 sccm NH_3, 230-240 W plasma power, 10 Torr, 15 min. growth time. (c) The dependence of tube volume (approximated as a cylinder) shows a maximal volume at about 10 nm in catalyst thickness. (d) Tube length as a function plasma power which indicates at a power below about 140 W, tube growth rate decreases significantly. Growth conditions were 22 sccm C_2H_2, 90 sccm NH_3, 10 Torr, 9 nm Ni thickness, 6 min. growth time. The data obtained above represents an averaging over 30 tubes.

In summary, we have developed a method for using high throughput, nanomanufacturable techniques for the realization of single, vertically aligned tubes integrated into 3D nano-scale architectures. Top down techniques, such as the use of deep UV chemically amplified resists for small feature size resolution, optical lithography units that allow unprecedented control over layer-to-layer registration, ICP etching techniques that result in near vertical, high aspect ratio 3D nano-scale architectures, in conjunction with the use of materials that are structurally and chemically compatible with the high temperature CVD synthesis of our PECVD grown tubes, were all key elements to the realization of these architectures. Structural characterization of the tubes confirms that the tubes have a filamentous structure, where the graphite planes are inclined to the central axis, and that the tubes appear to be well adhered to the Si substrate. The wafer-scale techniques developed here should accelerate the integration of PECVD grown nanotubes for a wide variety of applications in electronics and sensing.

Downloaded From: https://www.spiedigitallibrary.org/conference-proceedings-of-spie on 5/30/2018 Terms of Use: https://www.spiedigitallibrary.org/terms-of-use

ACKNOWLEDGMENTS

We sincerely acknowledge Robert Kowalczyk for his assistance with the PECVD growth chamber and performing chamber upgrades as necessary, in addition to Dr. Choonsup Lee and Dr. Paul von Allmen for useful discussions. We would also like to thank Shelby Hutchins of the California Institute of Technology and Brian Peters of Agilent Technologies for the images taken in Fig. 6f and Fig. 6e, respectively. We also acknowledge the Kavli Nanoscience Institute at the California Institute of Technology for providing use of TEM sample preparation facilities. This research was carried out at the Jet Propulsion Laboratory, California Institute of Technology, under a contract with the National Aeronautics and Space Administration and was funded through the internal Research and Technology Development (R&TD) program.

REFERENCES

[1] J. Li, Q. Ye, A. Cassell, H. T. Ng, R. Stevens, J. Han, and M. Meyyappan, *Appl. Phys Lett.* **82**, 2491 (2003).
[2] A. Bachtold, P. Hadley, T. Nakanishi, and C. Dekker, Science **294**, 1317 (2001).
[3] C. Yu, S. Saha, J. Zhou, L. Shi, A. Cassel, B. A. Cruden, Q. Ngo, and J. Li, *Transactions of the ASME* **128**, 234 (2006).
[4] R. Saito, G. Dresselhaus, and M. S. Dresselhaus, Physical Properties of Carbon Nanotubes (London: Imperial College Press), 1998.
[5] S. Fan, M. G. Chapline, N. R. Franklin, T. W. Tombler, A. M. Cassell, and H. Dai, *Science* **283**, 512 (1999).
[6] Q. Ngo, B. A. Cruden, A. M. Cassell, G. Sims, M. Meyyappan, J. Li, and C. Y. Yang, *Nano Lett.* **4**, 2403 (2004).
[7] Z. F. Ren, Z. P. Huang, J. W. Xu, J. H. Wang, P. Bush, M. P. Siegal, and P. N. Provencio, *Science* **282**, 1105 (1998).
[8] D. Nolan, D. C. Lynch, and A. H. Cutler, *J. Phys. Chem. B* 102, 4165 (1998).
[9] A. V. Melechko, V. I. Merkulov, T. E. McKnight, M. A. Guillorn, K. L. Klein, D. H. Lowndes, and M. L. Simpson, *J. Appl. Phys.* **97**, 041301 (2005).
[10] K. B. K. Teo, S.B. Lee, M. Chhowalla, V. Semet, V. T. Binh, O. Groening, M. Castignolles, A. Loiseau, G. Pirio, P. Legagneux, D. Pribat, D. G. Hasko, H. Ahmed, G. A. J. Amaratunga and W. I. Milne, *Nanotech.* **14**, 204 (2003).
[11] H. Ito, *IBM J. Res. and Dev.* **45**, 683 (2001).
[12] A. B. Kaul, K. Megerian, P. von Allmen, and R. L. Baron, *Nanotech.* **20**, 075303 (2009).
[13] Z. P. Huang, D. Carnahan, J. Rybczynski, M. Giersig, M. Sennett, D. Z. Wang, J. G. Wen, K. Kempa, and Z. F. Ren, *Appl. Phys. Lett.* **82**, 460 (2003).
[14] F. Laermer and D. Schilp, "Method of anisotropic ally etching silicon," U.S. Patent 5 501 893.
[15] Tachi, K. Tsujimoto, and S. Okudaira, *Appl. Phys. Lett.* **52**, 616 (1988).
[16] S. Helveg, C. Lopez-Cartes, J. Sehested, P. Hansen, B. Clausen, J. Rostrup-Nielson, F. Abild-Pedersen and J. Norskov, *Nature* **427**, 426 (2004).
[17] Y. Ominami, Q. Ngo, A. J. Austin, *et al.*, *Appl. Phys. Lett.* **87**, 233105 (2005).
[18] S. Brinkmann, J-Y Kim, and J. R. Greer *Phys. Rev. Lett.* **100**, 155502 (2008); http://www.jrgreer.caltech.edu/
[19] O. Louchev, Y. Sato, and H. Kanda, *Appl. Phys. Lett.* **80**, 2752 (2002).
[20] M. Chhowalla, K. B. K. Teo, C. Ducati, N. L. Rupesinghe, G. A. J. Amaratunga, A. C. Ferrari, D. Roy, J. Robertson, and W. I. Milne, *J. of Appl. Phys.* **90**, 5308 (2001).

Downloaded From: https://www.spiedigitallibrary.org/conference-proceedings-of-spie on 5/30/2018 Terms of Use: https://www.spiedigitallibrary.org/terms-of-use